Pflugers Arch - Eur J Physiol (2009) 458:915–928
DOI 10.1007/s00424-009-0670-2

MUSCLE PHYSIOLOGY

Reciprocal amplification of ROS and Ca^{2+} signals in stressed *mdx* dystrophic skeletal muscle fibers

Vyacheslav M. Shkryl · Adriano S. Martins · Nina D. Ullrich · Martha C. Nowycky · Ernst Niggli · Natalia Shirokova

Received: 27 November 2008 / Revised: 26 March 2009 / Accepted: 31 March 2009 / Published online: 22 April 2009

Abstract Muscular dystrophies are among the most severe inherited muscle diseases. The genetic defect is a mutation in the gene for dystrophin, a cytoskeletal protein which protects muscle cells from mechanical damage. Mechanical stress, applied as osmotic shock, elicits an abnormal surge of Ca^{2+} spark-like events in skeletal muscle fibers from dystrophin deficient (*mdx*) mice. Previous studies suggested a link between changes in the intracellular redox environment and appearance of Ca^{2+} sparks in normal mammalian skeletal muscle. Here, we tested whether the exaggerated Ca^{2+} responses in *mdx* fibers are related to oxidative stress. Localized intracellular and mitochondrial Ca^{2+} transients, as well as ROS production, were assessed with confocal microscopy. The rate of basal cellular but not mitochondrial ROS generation was significantly higher in *mdx* cells. This difference was abolished by pre-incubation of *mdx* fibers with an inhibitor of NAD(P)H oxidase. In addition, immunoblotting showed a significantly stronger expression of NAD(P)H oxidase in *mdx* muscle, suggesting a major contribution of this enzyme to oxidative stress in *mdx* fibers. Osmotic shock produced an abnormal and persistent Ca^{2+} spark activity, which was suppressed by ROS-reducing agents and by inhibitors of NAD(P)H oxidase. These Ca^{2+} signals resulted in mitochondrial Ca^{2+} accumulation in *mdx* fibers and an additional boost in cellular and mitochondrial ROS production. Taken together, our results indicate that the excessive ROS production and the simultaneous activation of abnormal Ca^{2+} signals amplify each other, finally culminating in a vicious cycle of damaging events, which may contribute to the abnormal stress sensitivity in dystrophic skeletal muscle.

Keywords Ca^{2+} sparks · Skeletal muscle · *mdx* mice · ROS · Confocal microscopy

Introduction

Dystrophinopathies are a category of muscle diseases that result from mutations of the dystrophin gene. This gene is located on chromosome Xp21 and encodes the protein dystrophin, which links the cytoskeleton with the extracellular matrix. The lack of dystrophin is thought to make the sarcolemma of skeletal muscle fibers and cardiac myocytes more fragile and more vulnerable to mechanical stress during contraction or eccentric stretch [19, 23]. Duchenne Muscular Dystrophy (DMD) is the most common muscular dystrophy. It is characterized by progressive muscle weakness, deterioration of skeletal and cardiac muscle function, and premature death. *mdx* mice completely lack dystrophin and recapitulate several of the pathophysiological features of DMD. Skeletal muscle from *mdx* mice shows signs of extensive muscle degeneration at the age of

Drs. V.M. Shkryl and A.S. Martins contributed equally to this work.

V. M. Shkryl · A. S. Martins · M. C. Nowycky · N. Shirokova (✉)
Department of Pharmacology and Physiology,
University of Medicine and Dentistry of New Jersey,
New Jersey Medical School, 185 South Orange Avenue,
Newark, NJ 07103, USA
e-mail: nshiroko@umdnj.edu

N. D. Ullrich · E. Niggli
Department of Physiology, University of Bern,
Bühlplatz 5,
Bern 3012, Switzerland

Present Address:
V. M. Shkryl
Department of Molecular Biophysics and Physiology,
Rush University,
Chicago 60612, USA

4–12 weeks. The skeletal muscle performance is later improved, at least to some extent, in older animals, presumably because of the upregulation and redistribution of utrophin, another cytoskeletal protein which can partly substitute for dystrophin [13]. The cardiac manifestations of the disease, however, become progressively more severe with age, finally resulting in dilated cardiac hypertrophy in ~10–12 month old animals [37]. *mdx* mice are widely used to elucidate the cellular mechanisms underlying the development of skeletal and cardiac muscle dysfunction in DMD and also to test possible therapeutic approaches to treat the disease [9, 32, 51, 52].

Several studies on muscle fibers from *mdx* mice indicated a disproportionate stretch-induced Ca^{2+} influx and abnormal intracellular Ca^{2+} homeostasis. It has been suggested that the lack of dystrophin results in an exaggerated fragility of the sarcolemma and in excessive Ca^{2+} influx via a number of voltage-independent pathways, such as "leak" channels" [31], stretch-activated channels (SAC, [53]), store operated channels (SOC, [49]) and microruptures [52]. However, although stretch-induced Ca^{2+} influx is greater in *mdx* cells than in cells from wild-type mice, it is still relatively small [12, 26]. This modest Ca^{2+} influx by itself does not appear to be sufficient to explain the excessive and potentially damaging intracellular Ca^{2+} signals evoked by mechanical stress, applied as osmotic shock in both *mdx* skeletal muscle fibers and in *mdx* ventricular cardiac myocytes [26, 49]. Therefore, it is likely that additional mechanisms are involved in the generation and further amplification of intracellular Ca^{2+} signals which ultimately lead to activation of Ca^{2+} dependent proteases and cell death (reviewed in [2]).

There are indications that oxidative stress (alone or in combination with mechanical load) can contribute to dystrophinopathy (reviewed in [46]). In both muscle fibers from DMD patients and *mdx* mice, the levels of most antioxidant enzymes and antioxidants are significantly elevated [4, 16]. Basal or background generation of reactive oxygen species (ROS) and reactive nitrogen species (RNS) seem to be elevated as well [51]. Oxidative stress is already present in young animals when muscle damage cannot yet be detected [14], suggesting that oxidative stress precedes the development of the disease. In addition, in vivo treatment of *mdx* mice with antioxidants, such as green tea extract [9] or *N*-acetylcysteine [51], improves skeletal muscle pathology and partially restores muscle force production.

Ca^{2+} entry via any of the suspected pathways mentioned above may stimulate production of ROS and RNS by several cellular mechanisms, including mitochondria [34], NAD(P)H oxidase [30], nitric oxide syntase (NOS) etc. Undue ROS production and accumulation may in turn lead to additional Ca^{2+} influx by increasing sarcolemmal Ca^{2+} permeability via lipid peroxidation, or by oxidation of proteins involved in other Ca^{2+} influx pathways, such as TRP channels (possible constituents of SAC and SOC [2, 21, 48]. ROS/RNS can also promote the release of Ca^{2+} from the sarcoplasmic reticulum (SR) via Ca^{2+} release channels (ryanodine receptors, RyRs), which are subject to oxidative/nitrositive modifications [29, 45]. Ca^{2+} released from the SR can subsequently further amplify the production of ROS thus establishing another intracellular positive feedback loop for damaging Ca^{2+} and ROS signals.

Our recent studies indicate that ROS contribute to the development of intracellular Ca^{2+} signals (reminiscent of Ca^{2+} sparks) induced by osmotic stress in normal mammalian skeletal muscle [30]. Ca^{2+} sparks are highly localized signals that are created by the opening and closing of a small group of RyRs. They are believed to reflect activation of RyRs by Ca^{2+}, and therefore represent "elementary events" of Ca^{2+}-induced Ca^{2+} release [35]. Unlike many other muscle types, mammalian skeletal muscle does not generate spontaneous Ca^{2+} sparks under physiological conditions [42]. The release of Ca^{2+} from the SR during excitation–contraction coupling (ECC) appears to be exclusively under the control of the voltage sensors (a.k.a., dihydropyridine receptors, DHPRs). Pathophysiological stimuli, however, such as strenuous exercise or mechanical stretch of the sarcolemma caused by osmotic shock, uncover spontaneous Ca^{2+} signals reminiscent of Ca^{2+} sparks. Compared to cells from healthy control animals, this activity seems to be abnormally augmented in muscle fibers dissected from *mdx* mice [49]. Here, we addressed the following questions: (1) is excessive "Ca^{2+} spark" activity in dystrophic *mdx* muscle fibers associated with, and possibly caused by, an enhanced ROS/RNS production? (2) Can ROS scavengers inhibit stress-induced "Ca^{2+} sparks"? (3) What are the sources of ROS/RNS in *mdx* skeletal muscle fibers?

Preliminary results of these studies have been published as an abstract [43].

Materials and methods

Fiber preparation

Male *mdx* (C57BL/10ScSn-*mdx*) mice at 4–8 weeks of age were purchased from Jackson Laboratory (Bar Harbor, Main, USA) or were provided by Drs. M. Rüegg (Biozentrum, University of Basel, Switzerland) and U. Rüegg (University of Geneva, Switzerland). Muscle fibers were enzymatically isolated from *flexor digitorium brevis* (FDB) muscle as previously described [30]. Briefly, mice were killed by cervical dislocation under deep anesthesia induced by intra-peritoneal injection of sodium pentobarbital (100 mg kg body weight^{-1}). FDB muscle was mechanically

dissected and incubated in a modified Tyrode solution (in mM, 145 NaCl, 5 KCl, 1 $CaCl_2$, 10 HEPES, 10 glucose, pH=7.0) supplemented with 2 mg ml^{-1} collagenase (Type I, Sigma, St. Louis, MO, USA) at 37°C for 40 min. Single fibers were obtained by gentle trituration of the digested muscles. They were plated on laminin-coated coverslips and studied 2–8 h after isolation. The procedure conforms with the *Guide for the Care and Use of Laboratory Animals* published by the US National Institutes of Health (NIH Publication No. 85-23, revised 1996).

Solutions

The isotonic external solution contained in mM, 140 NaCl, 5 KCl, 2.5 $CaCl_2$, 1 $MgCl_2$, 10 HEPES, 10 glucose. Its osmolality was ~300 mosmol kg^{-1} and pH of 7.0. The hypotonic solution contained in mM: 70 NaCl, 5 KCl, 2.5 $CaCl_2$, 1 $MgCl_2$, 10 HEPES, 10 glucose, with osmolality of ~170 mosmol kg^{-1}, and pH of 7.0. Most chemicals were obtained from Sigma (St. Louis, MO, USA). MnTBAP and Mn-cpx3, and NAD(P)H oxidase inhibitor diphenyleneiodonium (DPI) were from Calbiochem (EMD Chemicals, Gibbstown, NJ, USA).

Confocal imaging

To monitor microscopic intracellular Ca^{2+} transients, fibers were loaded with 10 μM fluorescent Ca^{2+} indicator fluo-4 AM (acetoxymethyl form of fluo-4) for 40 min. To follow local changes in intracellular and/or mitochondrial ROS/RNS production, cells were loaded with either 10 μM CM-H_2DCFDA (5-(and-6)-chloromethyl-2′,7′-dichlorodihydrofluorescein diacetate) or 5 μM MitoSOX red for 30 min. To examine changes in mitochondrial Ca^{2+} load, fibers were incubated with 10 μM mag-rhod-2 for 30 min. Voltage-sensitive indicators JC-1 (2 μM, 60 min) and TMRE (100 nM, 30 min) were used to monitor mitochondrial membrane potential. All probes were obtained from Molecular Probes (Invitrogen, Carlsbad, CA, USA). The fluorescence images (*X–Y* scans) were acquired with a laser-scanning confocal microscope (Radiance 2000; BioRad) connected to a Zeiss Axiovert 100 inverted microscope equipped with a 63x, 1.2 N.A. water immersion lens (Zeiss Inc., Oberkochen, Germany). Fluo-4, CM-H_2DCFDA and JC-1 were excited with the 488 nm and MitoSOX with the 514 nm lines of an Argon laser. Fluorescence emission was collected with 500 LP and 590/70 BP filters for fluo-4 and CM-H_2DCFDA, respectively. The relative contribution of red (aggregated) and green (monomeric) forms of JC-1 was determined as a ratio of fluorescence signals detected with 515/30 BP and 570 LP emission filters. Mag-rhod-2 and TMRE were excited with a HeNe laser at 543 nm. The emitted light was collected above 570 nm. In all experiments, the laser power was minimized and detection sensitivity was maximized in order to reduce the laser-light-induced production of ROS. In most experiments, 100 or 150 images (102.8 μm by 102.8 μm) were collected from the same spatial locus within a fiber at 0.1 Hz. Even though *X–Y* imaging does not provide sufficient information about the temporal properties of discrete events of Ca^{2+} release, we referred to them as Ca^{2+} sparks.

Sample preparation and Western blotting

Protein expression studies were conducted on explanted striated muscles from control and *mdx* mice as described previously [17]. Samples were snap-frozen in liquid nitrogen. After mechanical homogenization, tissue samples were lysed in SB20 (0.1 M Tris–HCl, pH 6.8, 20% SDS, 10 mM EDTA) and sonicated. Protein content was assayed using the Micro BCA protein assay kit (Pierce Biotechnology, Rockford, IL, USA). All samples were stored at −20°C. For immunoblotting, 20 μg of total protein were loaded per lane. Samples were run on 10% SDS-polyacrylamide gels and electrophoretically transferred to PVDF membranes (0.45 μM, Immobilon-P, Millipore, Bedford, MA, USA). Membranes were blocked in 5% non-fat dry milk in Tris-buffered saline-Tween 20, and then incubated with primary antibody against human NAD(P)H oxidase (rabbit anti-human gp91-phox, 1:200, Millipore, Bedford, MA, USA). Horseradish peroxidase (HRP) conjugated goat anti-rabbit IgG (1:1,000, Millipore, Bedford, MA, USA) was used as secondary antibody. Immunoreactivity of blots was detected using enhanced chemiluminescence (BioRad, Hercules, CA, USA). Immunoreaction against actin (goat polyclonal IgG, sc-1615, 1:2000, and HRP-conjugated donkey anti-goat IgG, sc-2020, 1:2000, Santa Cruz Biotechnology, CA, USA) served as internal control for protein expression levels. Quantification of Western blots was done by densitometric analysis of the membranes. Data are expressed as the mean signal ratio of NAD(P)H oxidase and actin in control and *mdx* tissue.

Statistical analysis

Data analysis is presented as mean±SEM. Statistical significance was determined by using Student's *t* test. In the figures * indicates $p<0.05$, ** indicates $p<0.01$. *n* and *N* indicate number of cells and animals studied in each group of experiments.

Results

Dystrophic skeletal muscle exhibits more pronounced intracellular Ca^{2+} signals in response to osmotic shock than muscle from control animals. Our previous results had

suggested a close link between the intracellular level of ROS and the development of Ca^{2+} sparks in both permeabilized and intact skeletal muscle fibers isolated from normal animals [24, 25, 30]. Here, we tested the hypothesis that sustained and/or transient oxidative stress in *mdx* muscle fibers underlies their more prominent intracellular Ca^{2+} responses triggered by mechanical challenges involving osmotic shocks. We also determined possible sources responsible for the increased generation of ROS, and possibly RNS, in *mdx* muscle fibers.

Stress-induced sparks often propagate inside the *mdx* muscle fibers

Wang et al. [49] recently reported that both hypo- and hyper-osmotic shock produced a long-lasting surge of Ca^{2+} sparks in skeletal muscle fibers from *mdx* mice. In contrast to the general responses observed in normal (a.k.a., wild type, WT) cells, where Ca^{2+} sparks were mostly restricted to a narrow space ~10 μm beneath the sarcolemma, response in *mdx* fibers propagated gradually throughout the entire cytosol. Figure 1a illustrates images from an *mdx* fiber before (image at 1.1 min), during (image at 2.6 min) and after (images at 4.0, 4.7, 6.3, and 21.3 min) a hypo-osmotic shock was applied. In 97% of *mdx* fibers (33 out of 34 fibers from N=11 animals) studied in this group, the osmotic shock triggered Ca^{2+} sparks. In nine cells (or in 38% of the responding cells), Ca^{2+} sparks rapidly propagated inside the fiber, reaching the center on average within 34.4±8.5 s (as seen on panel a). This is significantly different from the responses obtained in wild-type cells, where Ca^{2+} sparks were mostly localized to the sub-sarcolemmal region ([30] and Fig. 1c). It should be mentioned, that the pattern of intracellular Ca^{2+} responses

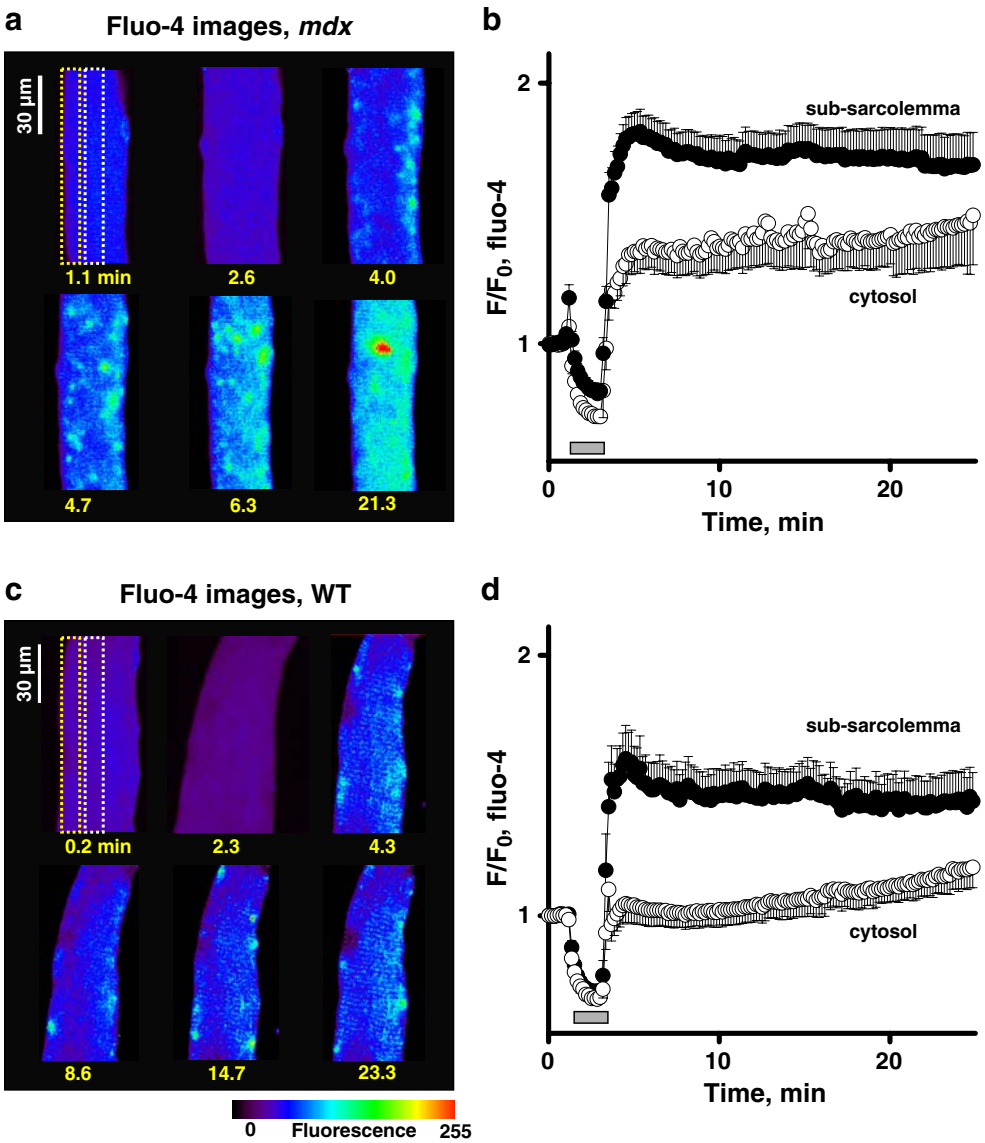

Fig. 1 Cytosolic Ca^{2+} signals elicited by hyposmotic shock in *mdx* and normal (*WT*) muscle fibers. Selected images of fluo-4 fluorescence in *mdx* (**a**) and WT (**c**) fiber before (images at 1.1 and 0.2 min, respectively) during (images at 2.6 and 2.3 min) and after osmotic shock was applied. *Boxes* indicate the regions where the average fluorescence was determined. **b**, **d** Averaged sub-sarcolemmal (*black circles*) and cytosolic (*white circles*) Ca^{2+} responses of 34 *mdx* and nine WT cells to osmotic shock

to stress (propagation or no propagation) varied in *mdx* fibers isolated from the same animal, probably because fibers are heterogeneously affected by the disease. To quantify and compare data obtained in different cells, we determined the spatial average fluorescence within 10 μm under the sarcolemma (yellow dashed box in panel a) or inside the fiber (white box) for each image in a series ($F(t)$). Then we normalized these signals to the average signal recorded before the osmotic shock was applied ($F(t)/F_0$). The corresponding $F(t)/F_0$ function represents the time dependence of changes in fluorescence in the selected region of interest. Figure 1b and d illustrate the averaged Ca^{2+} responses in the sub-sarcolemmal region (black circles) and in the center (white circles) of 34 *mdx* and nine WT muscle fibers studied in this series.

ROS/RNS generation is greater in *mdx* cells

In the literature, there are several reports of sustained oxidative stress in *mdx* skeletal muscle [16, 46, 51]. In addition, our previous data suggest that osmotic shock increases ROS production in wild-type cells [30]. Here, we tested (1) whether the "basal" production of ROS/RNS is elevated in dystrophic muscle fibers in *mdx*, compared with wild-type cells, and (2) whether an osmotic shock further increased ROS/RNS generation.

Fibers were loaded with CM-H_2DCFDA and imaged while being subjected to an osmotic shock. Inside the cell, CM-H_2DCFDA is hydrolysed to DCFH, which is oxidized by hydrogen peroxide or peroxynitrite to form the highly fluorescent compound DCF. Therefore, changes (i.e., increases) in DCF fluorescence are directly related to elevations in ROS/RNS concentration within a cell. Figure 2a shows images of DCF fluorescence in an *mdx* muscle fiber before (image at 1 min), during (image at 6 min) and after a hypo-osmotic (images at 8, 9, 10 and 12 min) shock was applied. Please note that the increase in fluorescence was initially mostly visible in the sub-sarcolemmal regions (images at 8 and 9 min) but later became more pronounced inside the fiber. Figure 2b represents averaged normalized changes in DCF signals in seven *mdx* fibers (N=3) subjected to osmotic shock (gray

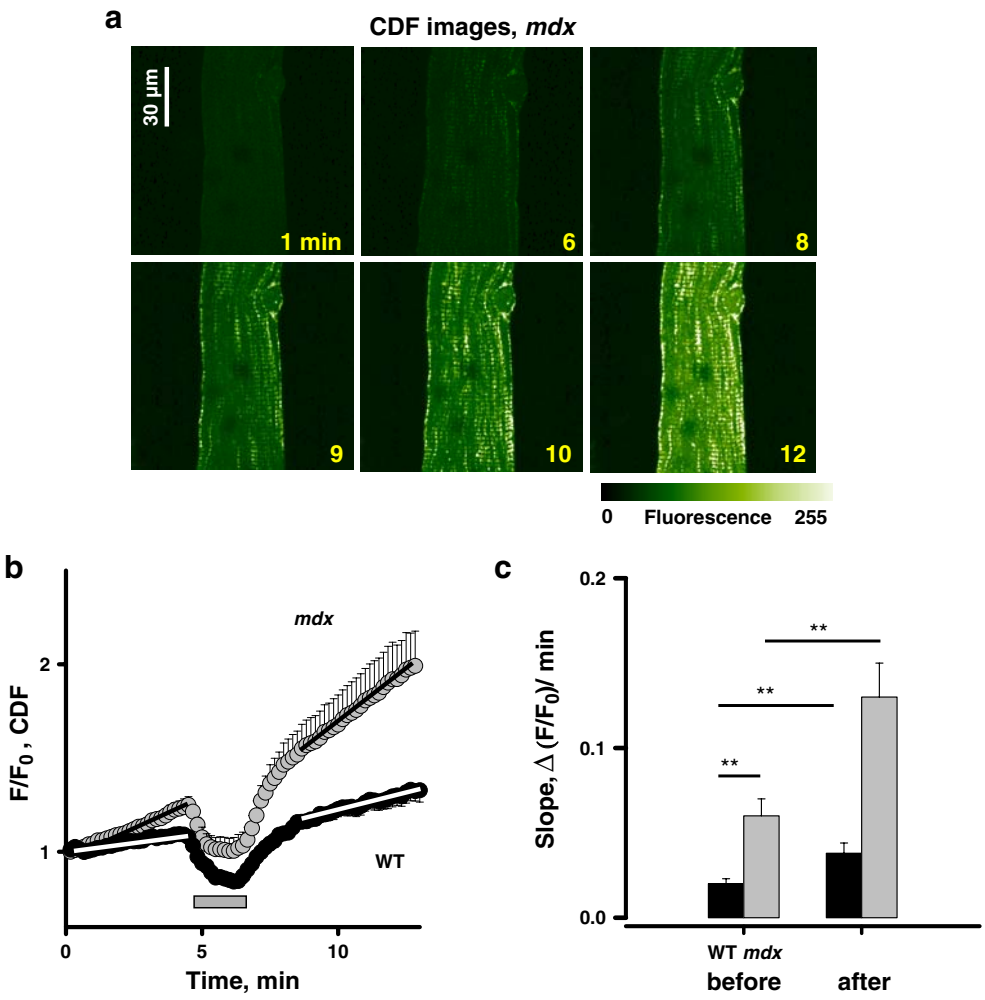

Fig. 2 Basal and stress-induced generation of ROS/RNS in skeletal muscle. **a** Selected images of DCF fluorescence in *mdx* fiber before (image at 1 min), during (image at 6 min) and after (images at 8, 9, 10, and 12 min) osmotic shock was applied. **b** Averaged DCF fluorescence from seven *mdx* cells (gray circles) and eight fibers from WT mice (*black circles*). **c** Averaged slopes of DCF signals before and after osmotic shock in *mdx* (*gray bars*) and WT cells (*black bars*). Steeper slopes indicate larger production of ROS/RNS in *mdx*

circles). Black circles represent changes in DCF fluorescence in eight cells from normal mice (N=4) studied in parallel with the same experimental protocol and confocal microscope settings. During these experiments, the DCF signal increased in both types of cells. The slope of the DCF fluorescence before the shock was applied reflects the rate of basal or endogenous generation of free radicals that lead to the oxidation of the indicator. The slope was significantly steeper after the shock suggesting an additional increase in ROS/RNS production. For each cell, the DCF recordings were fitted with linear functions before and after the osmotic shock was applied. The results are summarized in Fig. 2c. On average, the steepness before the shock was significantly (P<0.01) larger in *mdx* (gray bars) compared with WT (black bars) cells (0.06±0.01 and 0.02±0.003, respectively). The steepness significantly increased following the shock (0.13±0.02 and 0.04±0.01 in *mdx* and WT cells, respectively). The change of slope was somewhat more pronounced in *mdx* fibers (the slope ratios after/before were 2.16±0.01 and 2.00±0.01 in *mdx* and control cells, respectively). Because the slope of the DCF signal reflects the rate of generation of ROS/RNS, these results suggest (1) increased basal generation of free radicals and (2) greater increase in ROS/RNS production caused by osmotic challenge in *mdx* fibers compared with normal cells.

ROS/RNS scavengers inhibit intracellular Ca^{2+} responses to osmotic shock

As already mentioned, our previous studies suggested a link between ROS and the development of Ca^{2+} sparks in both permeabilized and intact mammalian muscle fibers [24, 25, 30]. The findings described above indicate a higher level of background and inducible ROS/RNS generation in *mdx* skeletal muscle fibers. Since ROS/RNS can make the RyRs more Ca^{2+} sensitive, they may be responsible for the excessive intracellular Ca^{2+} responses in *mdx* fibers. Here, we tested whether pre-incubation of *mdx* fibers with exogenous ROS/RNS scavengers or SOD mimetics suppresses Ca^{2+} sparks induced by osmotic shock in *mdx* muscle.

Changes in sub-sarcolemmal fluo-4 fluorescence were monitored in a control group of *mdx* fibers (no scavengers added), in fibers following 30 and 60 min incubation with MnTBAP (50 μM), Mn-cpx 3 (4 μM) and TIRON (10 mM) and in cells 30 min after wash out of drugs. Previously [30], we showed that incubation of fibers from normal mice with MnTBAP significantly reduced the basal ROS/RNS levels and decreased ROS/RNS production following osmotic stress. Here, we used three different compounds with distinct chemical structures and scavenging profiles to ensure that the results obtained are not associated with possible non-specific actions of these scavengers.

Figure 3a illustrates averaged changes in fluorescence in *mdx* fibers studied in control (n=6, N=3), after 30 (n=7, N=3) and 60 (n=5, N=3) min of incubation with 50 μM MnTBAP, and 30 min after washout of the scavenger (n=6, N=3). The mean fluorescence signal was determined during the first 6 min after returning to the isotonic solution in each group of fibers. As shown in Fig. 3b, the abnormal Ca^{2+} activity was significantly (P<0.01) suppressed by the drug (from F/F_0 of 1.47±0.06 to 1.28±0.03 after 30 min pre-incubation and further to 1.02±0.005 after 60 min of pre-incubation), and was partially restored after washout of MnTBAP (to 1.21±0.04), confirming reversibility of the inhibition.

Qualitatively similar results were also obtained with the two other scavengers. Figure 3c and d show that both Mn-cpx3 and TIRON effectively and reversibly inhibited cytosolic Ca^{2+} responses to osmotic shock in *mdx* muscle.

Contribution of NAD(P)H oxidase to elevated ROS/RNS level and excessive intracellular Ca^{2+} responses to osmotic shock in mdx muscle

There are several intracellular sources producing ROS/RNS in skeletal muscle. Mitochondria, NAD(P)H oxidase (NOX), xanthine oxidase (XO), and nitric oxide synthase (NOS) are among them (reviewed in [40]). Our previous studies suggested a pivotal role of NAD(P)H oxidase in the increased ROS production after osmotic shock in WT mammalian skeletal muscle fibers. They also suggested a rather limited role of mitochondria, NOS and XO [30].

The larger ROS production in *mdx* cells seen in Fig. 2 can be explained (1) by an increased activity and/or expression of NAD(P)H oxidase, or (2) by the recruitment of additional sources of ROS, which are of limited importance in wild-type fibers. Our results support both possibilities.

First, we examined whether NAD(P)H oxidase expression is higher in *mdx* skeletal muscle. Western blotting was performed on lysates of control and *mdx* skeletal muscle. At equal protein loading, immunoreactivity of a protein with an apparent molecular mass of 75 kDa corresponding to a transmembrane subunit of the NAD(P)H oxidase ($gp91^{phox}$, or NOX2 in the most recent terminology) showed a dramatic increase in expression levels and reached near maximal reactivity in *mdx* compared with control samples. To ascertain whether the increase in immunoreactivity of this band of 75 kDa corresponded indeed to an increase in the actual expression levels of the protein, we performed simultaneous immunoprecipitation studies using anti-actin antibody on the same protein lysates. Assuming that the expression of actin, which precipitates at ~42 kDa, is unchanged in *mdx* when compared with control tissue, this test served as an internal control for quantification of the NAD(P)H oxidase signal responses. Signal ratios of

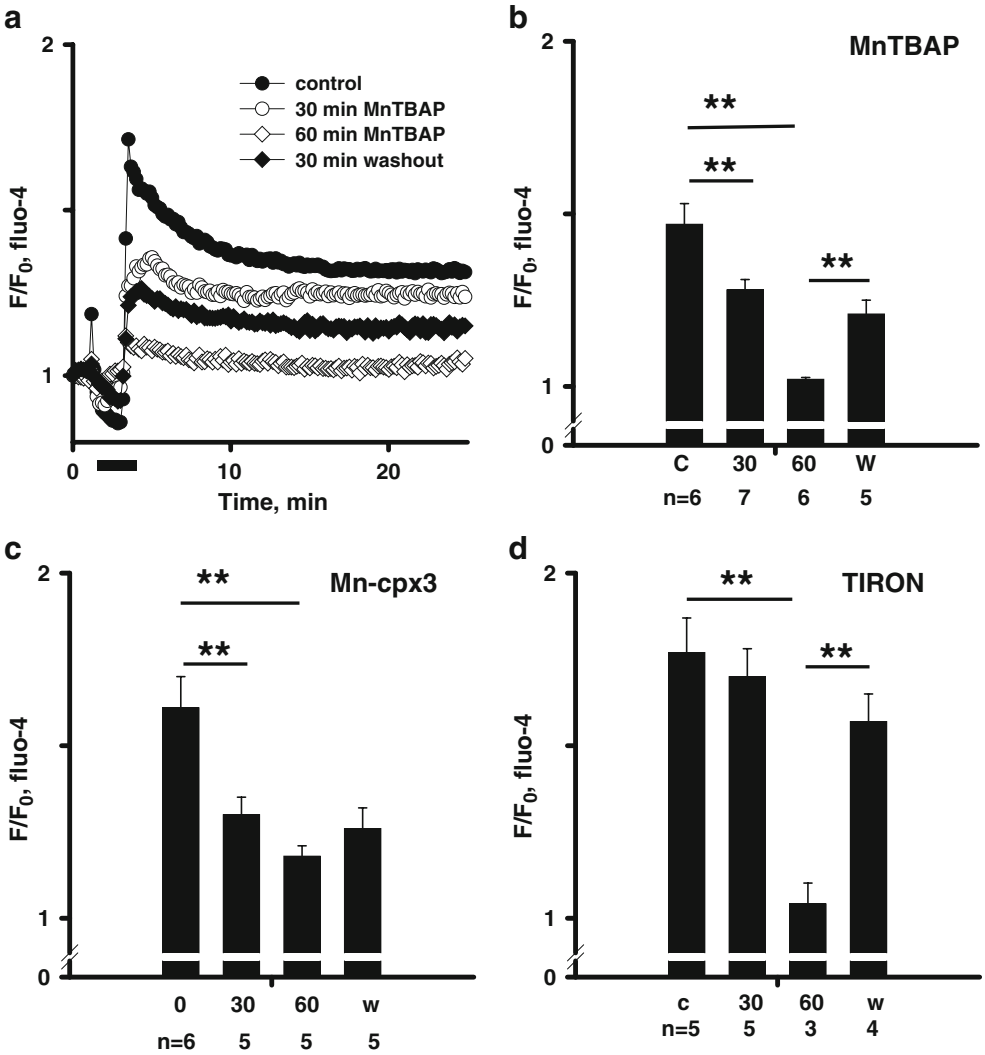

Fig. 3 ROS/RNS scavengers inhibit cytosolic Ca^{2+} responses to osmotic shock. **a** Average changes in normalized fluo-4 fluorescence in *mdx* fibers studied under control condition (no drugs added, *black circles*), 30 (*white circles*) and 60 min (*white diamonds*) after incubation with 50 μM MnTBAP, and after washout (*black diamonds*). **b** The mean fluorescence determined during the first 6 min after returning to the isotonic solution in each group of the experiments. **c**, **d** Summary of similar experiments but with Mn-cpx3 (4 μM) and TIRON (10 mM)

background-subtracted band intensities for $gp91^{phox}$ (at ~75 kDa) and actin (at ~42 kDa) in each lane were used for analysis. As shown in Fig. 4a, the expression of $gp91^{phox}$ is increased more than three fold in *mdx* skeletal muscle (N=7) when compared with control (N=3, P<0.01).

In skeletal muscle NAD(P)H oxidase is localized to the sarcolemma and T-tubular membrane and can be activated in a Ca^{2+}-dependent and Ca^{2+}-independent manner [22, 30]. Thus, NAD(P)H oxidase may be exposed to a microdomain of high [Ca^{2+}], which is established under the cell membrane by abnormal Ca^{2+} influx during regular mechanical activity of dystrophic muscle as well as during eccentric stretch. Therefore, ROS production by this enzyme can contribute to both the elevated basal level of ROS and the enhanced generation of free radicals following more severe mechanical challenges such as osmotic shock. Using CM-H_2DCFDA, we examined the rate of basal and stress-induced ROS generation in *mdx* cells pre-incubated for 30 min with 0.5 mM apocynin, an inhibitor of NAD(P)H oxidase. Apocynin significantly (P<0.05) reduced the basal level of ROS production (slopes of DCF curves before the shock were 0.03±0.005, n=10, N=4, in control, and 0.01±0.002, n=7, N=3, in apocynin, data not shown). The drug also nearly eliminated the increase in ROS generation by osmotic shock (slopes of DCF curves were 0.01±0.002 and 0.014±0.001, before and after the shock, respectively, data not shown). The variability in the baseline values of ROS/RNS levels in different groups of experiments is likely to be due to heterogeneity in the disease phenotype.

In the next group of experiments, fibers were loaded with the fluorescent Ca^{2+} indicator fluo-4 and incubated for 30 min with two different NAD(P)H oxidase inhibitors: apocynin (0.5 mM) and DPI (10 μM). As seen in Fig. 4b and c, both drugs significantly diminished cytosolic Ca^{2+} responses to osmotic shock. The mean fluorescence after returning to the isotonic solution was reduced from 1.8±0.04 in the control (n=8, N=6) to 1.25±0.06 (n=4, N=3) and 1.07±0.06 (n=5, N=3) in DPI and apocynin, respectively.

In Martins et al. [30], we suggested that activation of NOS and XO are not likely to account for stress-induced

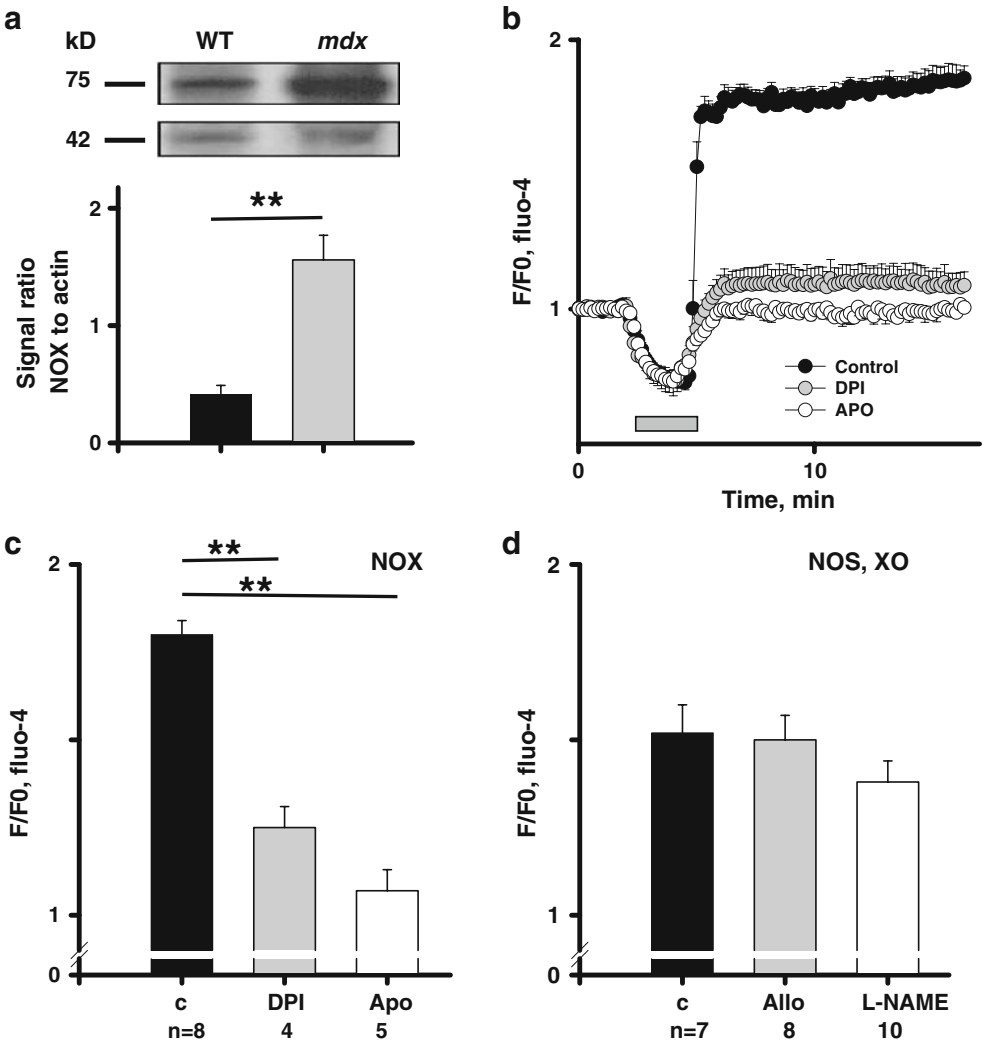

Fig. 4 NOX is a major contributor to the increased ROS production in *mdx* skeletal muscle. **a** Expression of NOX and actin in *mdx* and WT mice. *Top panel*, Western blots demonstrating protein levels of NOX and actin in two types of muscles. *Bottom level*, signal ratios of band intensities for $gp91^{phox}$ and actin in *mdx* (*gray bar*) and wild-type (*black bar*) muscles ($n=3$ animals for wild type, seven for *mdx*). **b** Average cytosolic Ca^{2+} responses to osmotic challenge in *mdx* fibers studied under control condition (no drugs added, *black circles*), and after incubation with NOX inhibitors apocynin (0.5 mM, *white circles*) and DPI (10 μM, *gray circles*). **c** The mean fluorescence determined during the first 6 min after returning to the isotonic solution in each group of the experiments illustrated in **b**. **d** The mean fluorescence after osmotic shock in control group fibers (*black bars*) and in cells pre-incubated with allopurinol (100 μM) and L-NAME (1 mM)

ROS production and cytosolic Ca^{2+} signals in normal muscle cells. Here, we also assessed the role of these sources in *mdx* muscle fibers. Figure 4d shows that the XO inhibitor allopurinol (100 μM) did not significantly change intracellular Ca^{2+} transients elicited by osmotic stress. The non-specific NOS inhibitor L-NAME (1 mM) somewhat reduced cytosolic Ca^{2+} responses but the reduction was not highly significant. The mean fluorescence was 1.52±0.08 ($n=5$, $N=3$) in control, 1.50±0.07 ($n=8$, $N=5$) after 30 min of incubation in XO inhibitor allopurinol and 1.38±0.06 ($n=10$, $N=4$) after 30 min exposure of fibers to NOS inhibitor L-NAME.

Overall, these data indicate that most likely NOX is the major contributor to the increase in ROS/RNS and augmented Ca^{2+} responses to osmotic shock in *mdx* skeletal muscle fibers.

Osmotic stress increases mitochondrial Ca^{2+} loading

Mitochondria are another potential source of ROS in skeletal muscle. It is known that muscle cells continuously generate ROS, as a byproduct of the respiratory chain, and that enhanced mitochondrial Ca^{2+} uptake stimulates further mitochondrial ATP and ROS production (reviewed in [8]). It is possible that stress-generated cytosolic Ca^{2+} is sequestered by mitochondria. In turn, this would stimulate mitochondrial ROS production, increase leakage of ROS to the cytosol and thus further amplify cytosolic Ca^{2+} signals. Here, we tested (1) whether and to what extent osmotic shock increases the mitochondrial Ca^{2+} load, and (2) whether the increase is different in *mdx* and wild-type muscle fibers.

Dystrophic *mdx* and normal muscle fibers were loaded with the low affinity Ca^{2+} indicator mag-rhod-2 in its AM ester form. Mag-rhod-2 is a charged molecule that preferentially partitions into the mitochondria. The dye has been demonstrated to be useful in studies of mitochondrial Ca^{2+} uptake in skeletal muscle, where the resting mitochondrial Ca^{2+} load seems to be quite high [44]. Figure 5a shows the mitochondrial mag-rhod-2 distribution and the fluorescence signal in an *mdx* cell before (image at 1 min), during (image at 4 min) and after the shock (images

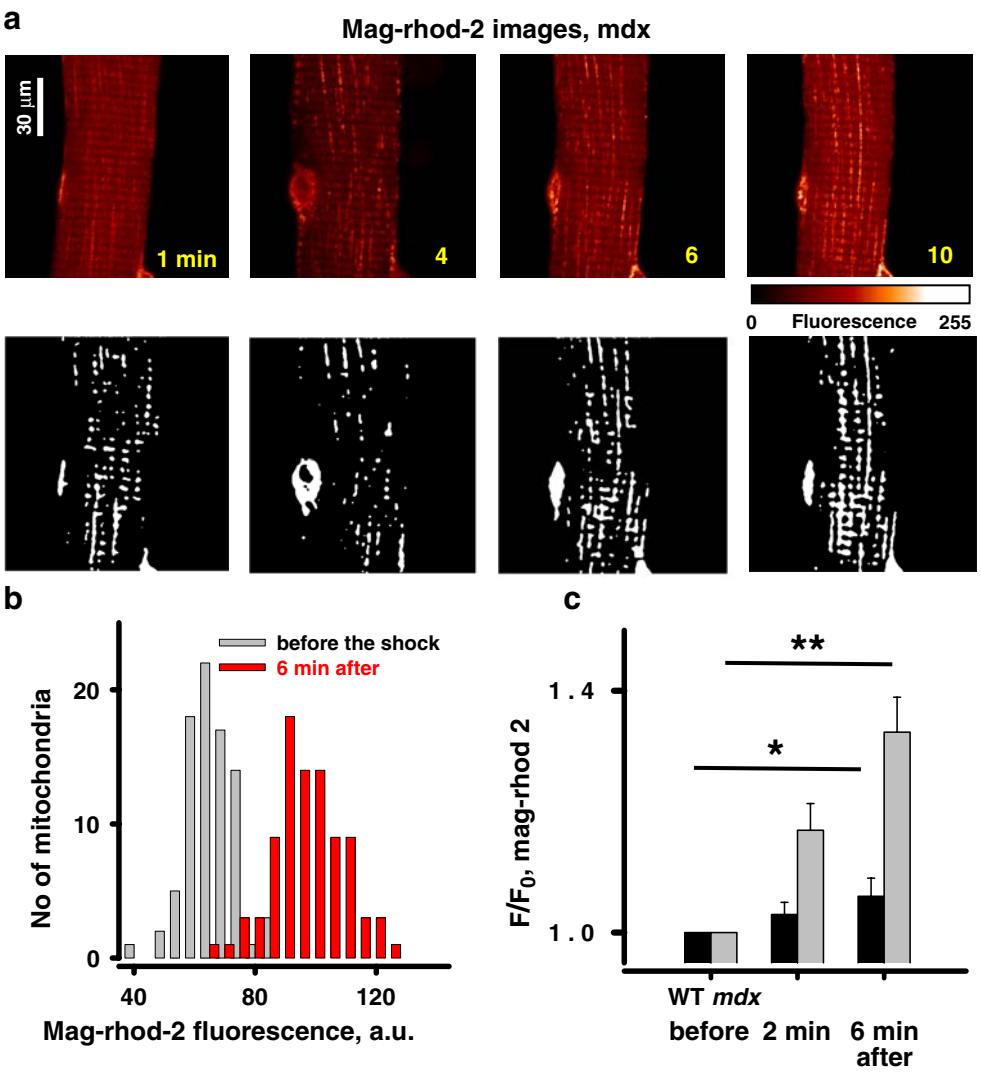

Fig. 5 Excessive cytosolic Ca^{2+} is taken up by mitochondria. **a** *Top panels* represent selected images of mag-rhod-2 fluorescence in an *mdx* cell before (image at 1 min), during (image at 4 min), and after (images at 6 and 10 min) osmotic shock was applied. *Bottom panels* show binary masks of mitochondria identified on corresponding mag-rhod-2 images. **b** Histogram of averaged fluorescence in the identified organelles before (*gray bars*) and 6 min after (*red bars*) osmotic shock was applied. **c** Average increase in mitochondrial Ca^{2+} related fluorescence after osmotic shock in *mdx* (*gray bars*) and wild-type (*black bars*) fibers

at 6 and 10 min). Mitochondria were identified in each image (as seen on binary masks at the bottom of panel a) and their average fluorescence was determined. Figure 5b shows the histogram of averaged fluorescence in the organelles before and 6 min after the osmotic shock was applied. In this particular fiber, the averaged mag-rhod-2 fluorescence (in a.u.) increased significantly ($P<0.01$) from 64.5±0.9 at resting conditions to 80.7±1.5 and 94.2±1.2 two and six min after the stress, respectively. Overall, in seven out of ten *mdx* fibers ($N=5$) osmotic shock produced a gradual and significant increase in mag-rhod-2 fluorescence (1.33±0.06 in units of F/F_0) at the end of the experiments (Fig. 5c). In contrast, in cells from normal mice, a significant increase in mitochondrial mag-rhod-2 signal was observed much less frequently (two out of 12 cells, $N=4$). It was substantially smaller than in *mdx* cells and preferentially detected in subsarcolemmal regions. The averaged mag-rhod-2 fluorescence increased from 69.2±1.6 at the beginning to 73.6±2.1 (in a.u.) at the end of experiments ($P<0.05$).

The larger mitochondrial Ca^{2+} accumulation in dystrophic fibers can be a direct consequence of enhanced cytosolic Ca^{2+} signals in these cells (as seen in Fig. 1), but also due to more sensitive mitochondrial Ca^{2+} uptake mechanism(s). Using mitochondrial and SR-targeted luminescent aequorins, Robert et al. [41] showed augmented mitochondrial Ca^{2+} signals resulting from similar cytosolic Ca^{2+} transients in *mdx* developing myotubes compared to WT, suggesting enhanced uptake in the *mdx* cells. As described below, our experiments support this possibility. Mag-rhod-2 is not a ratiometric fluorescent Ca^{2+} indicator. Therefore, direct quantitative comparison of the effectiveness of mitochondrial Ca^{2+} uptake is not feasible under our experimental conditions. Instead, we measured mitochondrial potential with the voltage-sensitive probe JC-1. JC-1 is an indicator that exhibits potential-dependent accumulation in mitochondria accompanied by a fluorescence emission shift from green to red. Muscle fibers were isolated from *mdx* and WT mice on the same day, loaded with 2 μM JC-1 for 60 min to

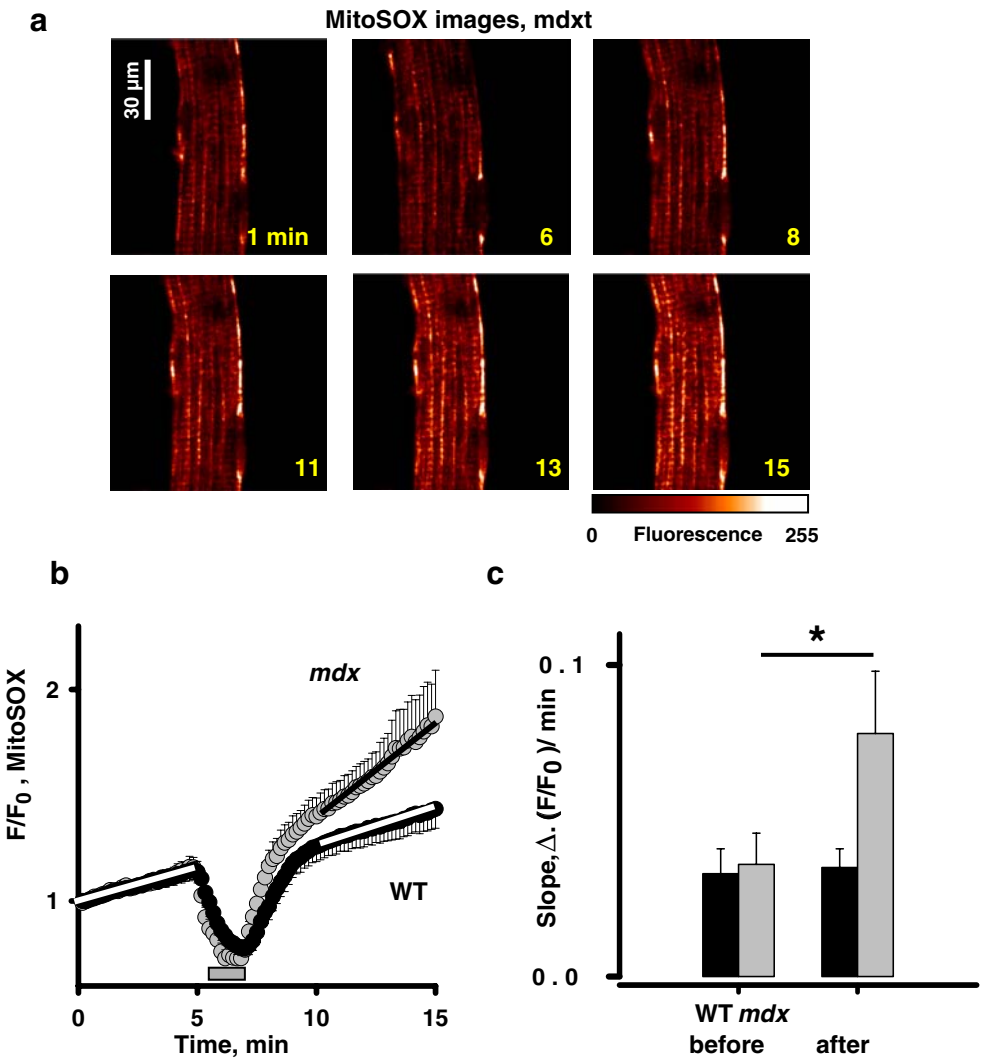

Fig. 6 Mitochondrial ROS production. **a** Selected images of MitoSOX fluorescence in an *mdx* cell before (image at 1 min), during (image at 6 min), and after (images at 8, 11, 13, and 15 min) osmotic shock was applied. **b** Averaged MitoSOX fluorescence from eight *mdx* cells (*gray circles*) and nine fibers from normal mice (*black circles*). **c** Averaged slopes of MitoSOX signals before and after osmotic shock in *mdx* (*gray bars*) and wild-type cells (*black bars*)

equilibrate dye distribution within the cell and studied in parallel. The red to green fluorescent ratio was significantly larger in *mdx* fibers (0.8±0.07, n=19, N=7 and 0.6±0.06, n=23, N=7 in *mdx* and WT cells, respectively), indicating that mitochondria in dystrophic fibers are hyperpolarized compared with those in WT. A larger potential gradient across the mitochondrial membrane could lead to stimulation of the electrogenic mitochondrial Ca^{2+} uniporter resulting in augmented mitochondrial Ca^{2+} accumulation in *mdx* skeletal muscle of this age group.

Osmotic stress increases mitochondrial ROS production

One of the consequences of moderate mitochondrial Ca^{2+} sequestration can be an enhancement of mitochondrial metabolism, as the activity of several enzymes of the TCA cycle depends on Ca^{2+}. Here, we directly measured mitochondrial ROS production in *mdx* and wild-type cells under identical experimental conditions. Fibers were loaded with the mitochondrial superoxide fluorescent probe MitoSOX red and imaged while subjected to hypo-osmotic shock. Because targeting of MitoSOX (and therefore the fluorescence signal intensity) is driven by the mitochondrial membrane potential, we also tested whether osmotic shocks can change this potential. As JC-1 is not very reliable for dynamic measurements, we used TMRE at a concentration of 100 nM, which we previously found to result in a non-quenching behavior in both skeletal muscle fibers and in cardiac myocytes [24, 26]. No significant changes of the TMRE fluorescence were elicited by osmotic shocks, neither in WT (n=5, N=3) nor in *mdx* (n=7, N=3) fibers, suggesting that the mitochondrial membrane potential did not change noticeably and that the MitoSOX signals reliably reflect mitochondrial ROS production. Figure 6a represents images of MitoSOX fluorescence in an *mdx* fiber before (image at 1 min) during (image at 6 min) and after (images at 8, 11, 13, and 15 min) a shock was applied. Averaged normalized MitoSOX fluorescence from eight *mdx* (N=6) fibers is shown on panel b (gray circles). As in the experiments with CM-H_2DCFDA, the MitoSOX curve was fitted with a linear

function before and after the shock was applied. As expected based on the results with mitochondrial Ca^{2+} measurements, there was a significant increase ($P<0.05$) in the slope of the curve (from 0.04±0.01 to 0.08±0.02). The increase clearly indicates an enhanced mitochondrial ROS generation resulting from the osmotic shock. Consistent with limited mitochondrial Ca^{2+} accumulation, no significant change in slope of the MitoSOX signal was detected in wild-type cells (black circles and bars, $n=9$, $N=4$). The slope only slightly changed from 0.033±0.008 to 0.035±0.006. Interestingly, the initial slope, which reflects the basal production of ROS by mitochondria, was slightly (but not significantly) larger in *mdx* cells. This suggests that, in contrast to NOX, mitochondria are likely to be minor contributor to basal oxidative stress in dystrophic skeletal muscle. However, they contribute to the increased ROS production in response to mechanical stress.

Discussion

Mechanical stress applied as an osmotic shock triggers a surge of Ca^{2+} spark-like events in intact skeletal muscle fibers. These events are not observed in intact mammalian muscle cells at rest or during physiological ECC. The extent of stress-induced intracellular Ca^{2+} activity is much greater in muscle fibers from *mdx* mice, but the reason for this difference is still elusive. Our previous studies on normal mammalian muscle strongly suggested a close link between overproduction of ROS/RNS and appearance of sparks in both permeabilized and intact fiber preparations. Here, we tested whether the exaggerated Ca^{2+} responses to osmotic challenges in dystrophic muscle are associated with (and presumably caused by) oxidative/nitrosative stress.

The present study revealed an elevated basal level of ROS in skeletal muscle fibers isolated from *mdx* mice, which is presumably mostly due to an enhanced ROS production by NOX. Our findings also revealed further consequences of this phenomenon. Challenging *mdx* fibers with mechanical stress, applied as osmotic shock, initiates several positive feedback loops. The mechanical challenge initially increases ROS production by NOX even further and triggers extensive intracellular Ca^{2+} transients. Subsequently, these large cytosolic Ca^{2+} responses lead to mitochondrial Ca^{2+} accumulation in *mdx* fibers and an additional boost in both NOX and mitochondrial ROS production which finally can again amplify cytosolic Ca^{2+} signals. Overall, our results suggest an important role for an abnormal production of ROS by NOX and mitochondria and consequent impaired Ca^{2+} homeostasis in pathological responses of dystrophic skeletal muscle to mechanical stress. Taken together, the present study shows that the near-simultaneous activation of several mutually synergistic feedback loops can culminate in a vicious cycle that may have damaging consequences for the affected muscle cells.

Oxidative/nitrosative stress and muscular dystrophy

In normally functioning healthy skeletal muscle, the basal production of ROS/RNS is balanced by various scavenging molecules and enzymes. Overproduction of free radicals and/or reduced ability of cellular defense mechanisms to neutralize them can eventually lead to sustained oxidative/nitrosative stress. Oxidative/nitrosative stress is involved in the pathogenesis of many skeletal muscle disorders and chronic diseases, such as muscle atrophy, fatigue, aging, diabetes, central core disease, malignant hyperthermia, etc. [18, 33].

Our present data show an increased basal level of ROS/RNS production in *mdx* muscle fibers (Fig. 2). We suggest that this is in large part due to the enhanced ROS generation by NAD(P)H oxidase. There are also some reports in the literature supporting the possibility that oxidative stress contributes to the pathology of muscular dystrophy. In particular, it has been reported that in dystrophic skeletal muscle (1) the levels of several antioxidant defense components such as catalase, glutathione peroxidase and superoxide dismutase are elevated; (2) the ROS concentration is increased [51]; and (3) levels of products of lipid peroxidation are higher (reviewed in [46]). In addition, although the expression of nNOS and, consequently, the production of NO have been found to be reduced in dystrophy [11, 50], the expression of iNOS has been recently shown to be increased [7]. Moreover, in vivo treatment of *mdx* mice with antioxidants can improve muscle function [9, 51]. Nevertheless, it is not yet clear to what extent oxidative/nitrosative stress determines the pathology of muscular dystrophy and what molecular pathways are involved. On one hand, levels of antioxidant enzymes are elevated in dystrophic muscle prior to the onset of muscle degeneration, suggesting that oxidative stress precedes the development of the disease [14]. On the other hand, these levels are also higher in extraocular skeletal muscle, which is spared from *mdx* pathology, and in dystrophic muscle already undergoing active regeneration [38, 39]. It is possible that oxidative/nitrosative stress itself does not drive muscle degeneration in dystrophy but rather acts synergistically with other factors, such as elevated resting Ca^{2+} concentrations, abnormal Ca^{2+} influx during repetitive muscle contraction and mechanical stress, to drive the pathological responses (e.g., [15]).

NOX as one of the major sources of oxidative stress in muscular dystrophy

A misbalance between the production of ROS/RNS and their elimination by various cellular scavenging systems may contribute to oxidative stress in dystrophy. Although

the levels of major antioxidants are higher in dystrophic muscle, they seem to be insufficient to prevent extensive ROS production by ROS-producing sources.

Our data suggest that NAD(P)H oxidase is likely to be one of the major sources of ROS behind the oxidative stress in dystrophy. NAD(P)H oxidase is a multimolecular complex containing two major transmembrane subunits (NOX and $p22^{phox}$) and several cytosolic regulatory subunits ($p47^{phox}$, $p40^{phox}$, $p67^{phox}$ and the small G proteins Rac1 or Rac2), which have to be translocated to the membrane to activate the oxidase. Skeletal muscle mostly expresses two isoforms of NOX, NOX2, and NOX4 [6, 10, 20]. Our results revealed that (1) expression of NOX2 (a.k.a. $gp91^{phox}$) is more than threefold higher in dystrophic skeletal muscle compared to normal mice and (2) incubation of dystrophic fibers with NOX inhibitors brings basal ROS production down close to the levels found in normal animals (Fig. 4). It seems that NOX, but not XO and NOS, is a primary source of ROS in response to the osmotic shock in muscle, as incubation of fibers with NOX inhibitors nearly eliminated the increase in ROS and cytosolic Ca^{2+} responses caused by the shock.

In Martins et al. [30] we had shown that activation of NOX following the mechanical challenge is partly governed by Ca^{2+}. Both NOX2 and NOX4 isoforms do not have an EF-hand like Ca^{2+} binding domains and therefore are unlikely to be directly activated by the increase in cytosolic $[Ca^{2+}]$. However, it has been suggested that Ca^{2+} can affect the activity of the NOX2 isoform indirectly via several pathways which are not mutually exclusive, involving Ca^{2+}-sensitive PKC isoforms, Ca^{2+}-dependent phospholipase A_2, association with S100 proteins, etc. (e.g., [1, 6, 10]). The activity of the NOX4 isoform does not seem to be regulated by Ca^{2+} [5], however more studies are needed to substantiate this conclusion.

Our experiments also revealed that in dystrophic cells, mitochondria are an important source of ROS generated subsequent to stress, in contrast to the situation in wild-type muscle. This is probably due to more severe cytosolic Ca^{2+} responses to osmotic shock in *mdx* fibers. Larger Ca^{2+} influx during mechanical stretch, increased resting $[Ca^{2+}]_c$ and/or increased sensitivity of RyR1 to be activated by Ca^{2+} as a result of oxidative/nitrosative stress (see below) can be responsible for this difference. Our results show that in *mdx* cells Ca^{2+} is eventually taken up by mitochondria (Fig. 5), stimulating ROS production by the organelles (Fig. 6).

Oxidative stress, Ca^{2+} influx, and intracellular Ca^{2+} homeostasis in muscular dystrophy

ROS/RNS have multiple targets in the sarcolemma and also inside the muscle cells. An increased level of free radicals can promote abnormal influx of Ca^{2+} into the muscle cells during muscle contraction or eccentric stretch by facilitating several possible Ca^{2+} influx pathways. Increased production of ROS may cause lipid peroxidation [14], and consequently may lead to additional Ca^{2+} influx via sarcolemmal membrane microruptures. Recently, some TRP channels have been shown to be sensitive to the cytosolic redox potential [21, 36]. As TRP channels are potential molecular components of SAC and SOC [2, 48], the oxidation of the cytosol may stimulate additional Ca^{2+} influx into the stressed cells via these channels as well.

ROS/RNS can also stimulate the release of Ca^{2+} from the SR via RyR1, as this molecule is a well-known target of oxidative/nitrosative modifications [45]. Increased levels of ROS/RNS may "hypersensitize" RyR1 making it more susceptible for activation by agonists, such as Ca^{2+}. In addition, *S*-nitrosylation and/or *S*-glutathionylation of RyR1 are likely to reduce binding of calstabin1 and calmodulin to RyR1, thereby relieving the inhibitory feedback on RyR1 exerted by these proteins [3, 7].

Taken together, production of ROS/RNS can intensify several mechanisms which deliver Ca^{2+} to the cytosolic space, both from the SR and from the extracellular space. This cytosolic Ca^{2+} load may, in turn, lead to additional production of ROS, thereby creating cross-talk to another positive feedback loop. For example, NOX can be further activated by Ca^{2+} [6, 10]. In addition, we found that mitochondria take up some of the extra Ca^{2+} load, which subsequently leads to an elevated generation of ROS by the mitochondria themselves.

Ca^{2+} overload and ROS production may have downstream consequences ranging far beyond the initial signaling events. For example, they may activate Ca^{2+}-dependent proteases, such as calpain, resulting in proteolysis of cellular constituents. In addition, they may lead to opening of the mitochondrial transition pore, allowing the efflux of proapoptotic mediators into the cytosol. Apoptotic and/or necrotic cell death may be one of the mechanisms leading to muscle wasting and fibrosis in patients with muscle dystrophy [47]. Sustained Ca^{2+} overload can eventually lead to the impaired mitochondrial oxidative phosphorylation reported in older *mdx* mice and DMD patients [27]. In addition, ROS can directly affect the contractile properties of muscle cells [28], also decreasing the force production in dystrophy.

In summary, one of the key findings of our study is that the near-simultaneous activation of two signaling systems triggers early events which synergistically contribute to the excessive stress sensitivity of dystrophic muscle. Based on this observation, one could consider the possibility to concurrently target both pathways, the Ca^{2+} signaling and the ROS generation, with pharmacological or other therapeutic approaches.

Acknowledgments This study was supported by the grants from NIH (to N.S.), Muscular Dystrophy Association (to N.S. and M.C.N.), Swiss Foundation for Research on Muscle Diseases (to E.N. and N.S.),

Swiss National Science Foundation (to E.N.) and UMDNJ and Sigrist Foundations (to N.S). We thank Dr. Philippe Beauchamp for technical help, and Drs. John Reeves, Roman Shirokov and Andrew Thomas for discussions.

References

1. Abramov AY, Jacobson J, Wientjes F, Hothersall J, Canevari L, Duchen MR (2005) Expression and modulation of an NADPH oxidase in mammalian astrocytes. J Neurosci 25:9176–9184
2. Allen DG, Whitehead NP, Yeung EW (2005) Mechanisms of stretch-induced muscle damage in normal and dystrophic muscle: role of ionic changes. J Physiol 567:723–735
3. Aracena P, Tang W, Hamilton SL, Hidalgo C (2005) Effects of *S*-glutathionylation and *S*-nitrosylation on calmodulin binding to triads and FKBP12 binding to type 1 calcium release channels. Antioxid Redox Signal 7:870–881
4. Austin L, de Niese M, McGregor A, Arthur H, Gurusinghe A, Gould MK (1992) Potential oxyradical damage and energy status in individual muscle fibres from degenerating muscle diseases. Neuromuscul Disord 2:27–33
5. Banfi B, Molnar G, Maturana A, Steger K, Hegedus B, Demaurex N, Krause KH (2001) A Ca^{2+}-activated NADPH oxidase in testis, spleen, and lymph nodes. J Biol Chem 276:37594–37601
6. Bedard K, Krause KH (2007) The NOX family of ROS-generating NADPH oxidases: physiology and pathophysiology. Physiol Rev 87:245–313
7. Bellinger AM, Reiken S, Carlson C, Mongillo M, Liu X, Rothman L, Matecki S, Lacampagne A, Marks AR (2009) Hypernitrosylated ryanodine receptor calcium release channels are leaky in dystrophic muscle. Nat Med 15:325–330
8. Brookes PS, Yoon Y, Robotham JL, Anders MW, Sheu SS (2004) Calcium, ATP, and ROS: a mitochondrial love-hate triangle. Am J Physiol Cell Physiol 287:C817–C833
9. Buetler TM, Renard M, Offord EA, Schneider H, Ruegg UT (2002) Green tea extract decreases muscle necrosis in *mdx* mice and protects against reactive oxygen species. Am J Clin Nutr 75:749–753
10. Cave AC, Brewer AC, Narayanapanicker A, Ray R, Grieve DJ, Walker S, Shah AM (2006) NADPH oxidases in cardiovascular health and disease. Antioxid Redox Signal 8:691–728
11. Chang WJ, Iannaccone ST, Lau KS, Masters BS, McCabe TJ, McMillan K, Padre RC, Spencer MJ, Tidball JG, Stull JT (1996) Neuronal nitric oxide synthase and dystrophin-deficient muscular dystrophy. Proc Natl Acad Sci USA 93:9142–9147
12. De Backer F, Vandebrouck C, Gailly P, Gillis JM (2002) Long-term study of Ca^{2+} homeostasis and of survival in collagenase-isolated muscle fibres from normal and *mdx* mice. J Physiol 542:855–865
13. Deconinck AE, Rafael JA, Skinner JA, Brown SC, Potter AC, Metzinger L, Watt DJ, Dickson JG, Tinsley JM, Davies KE (1997) Utrophin–dystrophin-deficient mice as a model for Duchenne muscular dystrophy. Cell 90:717–727
14. Disatnik MH, Dhawan J, Yu Y, Beal MF, Whirl MM, Franco AA, Rando TA (1998) Evidence of oxidative stress in *mdx* mouse muscle: studies of the pre-necrotic state. J Neurol Sci 161:77–84
15. Dudley RW, Danialou G, Govindaraju K, Lands L, Eidelman DE, Petrof BJ (2006) Sarcolemmal damage in dystrophin deficiency is modulated by synergistic interactions between mechanical and oxidative/nitrosative stresses. Am J Pathol 168:1276–1287
16. Dudley RW, Khairallah M, Mohammed S, Lands L, Des Rosiers C, Petrof BJ (2006) Dynamic responses of the glutathione system to acute oxidative stress in dystrophic mouse (mdx) muscles. Am J Physiol Regul Integr Comp Physiol 291:R704–R710
17. Dupont E, Matsushita T, Kaba RA, Vozzi C, Coppen SR, Khan N, Kaprielian R, Yacoub MH, Severs NJ (2001) Altered connexin expression in human congestive heart failure. J Mol Cell Cardiol 33:359–371
18. Durham WJ, Aracena-Parks P, Long C, Rossi AE, Goonasekera SA, Boncompagni S, Galvan DL, Gilman CP, Baker MR, Shirokova N, Protasi F, Dirksen R, Hamilton SL (2008) RyR1 S-nitrosylation underlies environmental heat stroke and sudden death in Y522S RyR1 knockin mice. Cell 133:53–65
19. Ervasti JM, Campbell KP (1993) Dystrophin and the membrane skeleton. Curr Opin Cell Biol 5:82–87
20. Espinosa A, Leiva A, Pena M, Muller M, Debandi A, Hidalgo C, Carrasco MA, Jaimovich E (2006) Myotube depolarization generates reactive oxygen species through NAD(P) H oxidase; ROS-elicited Ca^{2+} stimulates ERK, CREB, early genes. J Cell Physiol 209:379–388
21. Hara Y, Wakamori M, Ishii M, Maeno E, Nishida M, Yoshida T, Yamada H, Shimizu S, Mori E, Kudoh J, Shimizu N, Kurose H, Okada Y, Imoto K, Mori Y (2002) LTRPC2 Ca^{2+}-permeable channel activated by changes in redox status confers susceptibility to cell death. Mol Cell 9:163–173
22. Hidalgo C, Sanchez G, Barrientos G, Aracena-Parks P (2006) A transverse tubule NADPH oxidase activity stimulates calcium release from isolated triads via ryanodine receptor type 1 S -glutathionylation. J Biol Chem 281:26473–26482
23. Hoffman EP, Brown RH Jr, Kunkel LM (1987) Dystrophin: the protein product of the Duchenne muscular dystrophy locus. Cell 51:919–928
24. Isaeva EV, Shirokova N (2003) Metabolic regulation of Ca^{2+} release in permeabilized mammalian skeletal muscle fibres. J Physiol 547:453–462
25. Isaeva EV, Shkryl VM, Shirokova N (2005) Mitochondrial redox state and Ca^{2+} sparks in permeabilized mammalian skeletal muscle. J Physiol 565:855–872
26. Jung C, Martins AS, Niggli E, Shirokova N (2008) Dystrophic cardiomyopathy: amplification of cellular damage by Ca^{2+} signalling and reactive oxygen species-generating pathways. Cardiovasc Res 77:766–773
27. Kuznetsov AV, Winkler K, Wiedemann FR, von Bossanyi P, Dietzmann K, Kunz WS (1998) Impaired mitochondrial oxidative phosphorylation in skeletal muscle of the dystrophin-deficient *mdx* mouse. Mol Cell Biochem 183:87–96
28. Lamb GD, Posterino GS (2003) Effects of oxidation and reduction on contractile function in skeletal muscle fibres of the rat. J Physiol 546:149–163
29. Marks A, Vianna DM, Carrive P (2009) Non-shivering thermogenesis without interscapular brown adipose tissue involvement during conditioned fear in the rat. Am J Physiol Regul Integr Comp Physiol 296:R1239–1247
30. Martins AS, Shkryl VM, Nowycky MC, Shirokova N (2008) Reactive oxygen species contribute to Ca^{2+} signals produced by osmotic stress in mouse skeletal muscle fibres. J Physiol 586:197–210
31. McCarter GC, Steinhardt RA (2000) Increased activity of calcium leak channels caused by proteolysis near sarcolemmal ruptures. J Membr Biol 176:169–174
32. Millay DP, Sargent MA, Osinska H, Baines CP, Barton ER, Vuagniaux G, Sweeney HL, Robbins J, Molkentin JD (2008) Genetic and pharmacologic inhibition of mitochondrial-dependent necrosis attenuates muscular dystrophy. Nat Med 14:442–447
33. Moylan JS, Reid MB (2007) Oxidative stress, chronic disease, and muscle wasting. Muscle Nerve 35:411–429
34. Nethery D, Callahan LA, Stofan D, Mattera R, DiMarco A, Supinski G (2000) PLA2 dependence of diaphragm mitochondrial formation of reactive oxygen species. J Appl Physiol 89:72–80

35. Niggli E, Shirokova N (2007) A guide to sparkology: the taxonomy of elementary cellular Ca^{2+} signaling events. Cell Calcium 42:379–387
36. Poteser M, Graziani A, Rosker C, Eder P, Derler I, Kahr H, Zhu MX, Romanin C, Groschner K (2006) TRPC3 and TRPC4 associate to form a redox-sensitive cation channel. Evidence for expression of native TRPC3-TRPC4 heteromeric channels in endothelial cells. J Biol Chem 281:13588–13595
37. Quinlan JG, Hahn HS, Wong BL, Lorenz JN, Wenisch AS, Levin LS (2004) Evolution of the mdx mouse cardiomyopathy: physiological and morphological findings. Neuromuscul Disord 14:491–496
38. Ragusa RJ, Chow CK, Porter JD (1997) Oxidative stress as a potential pathogenic mechanism in an animal model of Duchenne muscular dystrophy. Neuromuscul Disord 7:379–386
39. Ragusa RJ, Chow CK, St Clair DK, Porter JD (1996) Extraocular, limb and diaphragm muscle group-specific antioxidant enzyme activity patterns in control and *mdx* mice. J Neurol Sci 139:180–186
40. Reid MB (2001) Redox modulation of skeletal muscle contraction: what we know and what we don't. J Appl Physiol 90:724–731
41. Robert V, Massimino ML, Tosello V, Marsault R, Cantini M, Sorrentino V, Pozzan T (2001) Alteration in calcium handling at the subcellular level in mdx myotubes. J Biol Chem 276:4647–4651
42. Shirokova N, Garcia J, Rios E (1998) Local calcium release in mammalian skeletal muscle. J Physiol 512:377–384
43. Shkryl VM, Shirokova N (2006) ROS scavengers inhibit stress-induced Ca^{2+} sparks in skeletal muscle fibers. Biophys J:67a
44. Shkryl VM, Shirokova N (2006) Transfer and tunneling of Ca^{2+} from sarcoplasmic reticulum to mitochondria in skeletal muscle. J Biol Chem 281:1547–1554
45. Stamler JS, Meissner G (2001) Physiology of nitric oxide in skeletal muscle. Physiol Rev 81:209–237
46. Tidball JG, Wehling-Henricks M (2007) The role of free radicals in the pathophysiology of muscular dystrophy. J Appl Physiol 102:1677–1686
47. Tidball JG, Albrecht DE, Lokensgard BE, Spencer MJ (1995) Apoptosis precedes necrosis of dystrophin-deficient muscle. J Cell Sci 108:2197–2204
48. Vandebrouck A, Sabourin J, Rivet J, Balghi H, Sebille S, Kitzis A, Raymond G, Cognard C, Bourmeyster N, Constantin B (2007) Regulation of capacitative calcium entries by alpha1-syntrophin: association of TRPC1 with dystrophin complex and the PDZ domain of alpha1-syntrophin. FASEB J 21:608–617
49. Wang X, Weisleder N, Collet C, Zhou J, Chu Y, Hirata Y, Zhao X, Pan Z, Brotto M, Cheng H, Ma J (2005) Uncontrolled calcium sparks act as a dystrophic signal for mammalian skeletal muscle. Nat Cell Biol 7:525–530
50. Wehling M, Spencer MJ, Tidball JG (2001) A nitric oxide synthase transgene ameliorates muscular dystrophy in *mdx* mice. J Cell Biol 155:123–131
51. Whitehead NP, Pham C, Gervasio OL, Allen DG (2008) N-Acetylcysteine ameliorates skeletal muscle pathophysiology in *mdx* mice. J Physiol 586:2003–2014
52. Yasuda S, Townsend D, Michele DE, Favre EG, Day SM, Metzger JM (2005) Dystrophic heart failure blocked by membrane sealant poloxamer. Nature 436:1025–1029
53. Yeung EW, Whitehead NP, Suchyna TM, Gottlieb PA, Sachs F, Allen DG (2005) Effects of stretch-activated channel blockers on $[Ca^{2+}]$i and muscle damage in the mdx mouse. J Physiol 562:367–380